Songklanakarin J. Sci. Technol.
42 (2), 371-382, Mar. - Apr. 2020

http://www.sjst.psu.ac.th

Original Article

Convective two-layered flow and temperature distribution through an inclined porous medium in a rotating system

Karuna Sree Chitturi[1*], Sri Ramachandra Murty Paramsetti[2], and Sobhan Babu Kappala[3]

[1] *Department of Mathematics, Vignan's Foundation for Science, Technology and Research, (Deemed to be University) Vadlamudi, Andhra Pradesh, 522213 India*

[2] *Department of Mathematics, GIS, Gitam (Deemed to be University), Visakhapatnam, Andhra Pradesh, 530045 India*

[3] *Department of Mathematics, University College of Engineering (Narasaraopet), Jawaharlal Nehru Technological University, Kakinada, Andhra Pradesh, 533003 India*

Received: 27 August 2018; Revised: 7 January 2019; Accepted: 9 January 2019

Abstract

The convective motion of two incompressible viscous fluids that are different in thermal conductivities, viscosities and densities with heat transfer aspects in a rotating inclined channel, in which the pressure gradient is kept constant, is studied. The two phases are occupied by two different homogeneous isotropic porous materials having different permeabilities. The flow is steady, laminar and fully developed. Due to the inclusion of buoyancy forces, viscous and Darcy dissipation terms, the governing equations are non-linear and coupled. The regular Perturbation Method is used to obtain their solutions. The effects of the governing parameters such as rotation parameter, porous parameter, angle of inclination, Grashof number, ratio of heights, the ratio of viscosities and the ratio of thermal conductivities on the fluid flow are discussed in detail. It is observed that an increase in the Coriolis force incorporated through rotation parameter reduces the temperature and primary velocity of the flow.

Keywords: two-layered flow, inclined channel, porous medium, rotating system, heat transfer

1. Introduction

The role of fluid flow and heat transfer in a system containing saturated porous medium has drawn great mathematical and practical interest for understanding the transport processes occurring in several engineering systems such as heat pipes, geothermal reservoirs and nuclear debris beds. Various problems in the field have been studied by many researchers, namely Beckermann, Viskanta, and Ramadhyani (1988), Bian, Vasseur, Bilgen, and Meng (1996), Chauhan and Rema (2005), Hayat, Husain, and Khan (2007), Rudraiah (1988), Seddeek (2002), Sunil and Mahajan (2009). Prasad (1991) studied convective flow interaction with temperature distribution in a composite channel partially filled with porous medium. Kuznetsov (1998) investigated the Couette flow between the fluid and porous layers. Rotating convection flow through the porous medium has been studied by Krishna, Prasad Rao, and Ramachandra Murthy (2002). Chauhan and Rashmi (2012a) studied magnetohydrodynamic (MHD) flow through a porous medium in a rotating channel taking Hall currents into account. Heat transfer effects on rotating MHD flow and rotating MHD Couette flow in a porous medium with Hall currents has been analyzed by Chauhan and Rastogi (2012). Lima, Assad, and Paiva (2016) have studied two-phase magneto convection flow with heat transfer in an inclined channel. Recently, Siva Reddy, Chamkha Ali, and Anjan Kumar (2017) have analyzed the thermal-diffusion and diffusion-thermo effects on MHD natural convection flow through a porous medium in a rotating system. Even though the study on convective flow and temperature distribution

*Corresponding author
Email address: karuna637@gmail.com

through porous medium with inclined geometry is useful in many areas particularly in geophysical systems, there appears to be a very limited number of researchers, notably Guven, Aytac, and Ibrahim (2012), Malashetty, Umavathi, and Kumar (2001), Simon and Shagaiya (2013), Sri Ramachandra Murty, and Balaji Prakash (2016), Sri Ramachandra Murty, Balaji Prakash, & Karuna Sree (2018). The purpose of the present study is to analyze the effects of the parameters such as inclination angle, rotation parameter and porous parameter etc., on MHD convective two-layered flow and heat transfer through an inclined porous medium in a rotating system. To obtain realistic predictions, we have considered Brinkman extended Darcy-Lapwood model following Malashetty, Umavathi, and Kumar (2001).

2. Materials and Methods

The physical representation of the problem is shown in Figure 1 It is composed of two inclined plates which are parallel and infinite in length along x and z-directions. Temperatures of the upper and lower plates, T_{w_1} and T_{w_2} are kept constant. 'Φ' is the angle made by the inclined channel with the horizontal plane. The regions $-h_2 \le y \le 0$ and $0 \le y \le h_1$ are loaded with two different homogeneous isotropic porous materials with different permeabilities. These two phases are filled with two different incompressible viscous fluids with different thermal conductivities, densities and viscosities. The two fluids have constant transport properties with laminar flow, and fully developed and are assumed to be in a steady state. The flow in the channel is navigated by a constant pressure gradient $\left(\frac{-\partial p}{\partial x}\right)$ and temperature gradient $\Delta T = T_{w_1} - T_{w_2}$.

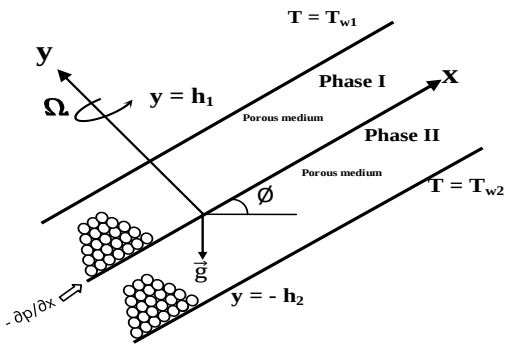

Figure 1. Physical configuration

With the angular velocity Ω, the entire system is rotated about the y-axis. Then the equations of motion and energy for Boussinesq fluids following Malashetty, Umavathi, and Kumar (2001) are:

Region-I

$$\mu_1 \frac{d^2 u_1}{dy^2} + \rho_1 g \beta_1 \sin\phi \left(T_1 - T_{w_2}\right) - \frac{\mu_1}{k_1} u_1 = \frac{\partial p}{\partial x} + 2\rho_1 \Omega w_1 \tag{1}$$

$$\mu_1 \frac{d^2 w_1}{dy^2} - \frac{\mu_1}{k_1} w_1 = -2\rho_1 \Omega u_1 \tag{2}$$

$$\frac{d^2 T_1}{dy^2} + \frac{\mu_1}{K_1}\left[\left(\frac{du_1}{dy}\right)^2 + \left(\frac{dw_1}{dy}\right)^2\right] + \frac{\mu_1}{K_1 k_1}\left(u_1^2 + w_1^2\right) = 0 \tag{3}$$

Region-II

$$\mu_2 \frac{d^2 u_2}{dy^2} + \rho_2 g \beta_2 \sin\phi \left(T_2 - T_{w_2}\right) - \frac{\mu_2}{k_2} u_2 = \frac{\partial p}{\partial x} + 2\rho_2 \Omega w_2 \tag{4}$$

$$\mu_2 \frac{d^2 w_2}{dy^2} - \frac{\mu_2}{k_2} w_2 = -2\rho_2 \Omega u_2 \tag{5}$$

$$\frac{d^2 T_2}{dy^2} + \frac{\mu_2}{K_2}\left[\left(\frac{du_2}{dy}\right)^2 + \left(\frac{dw_2}{dy}\right)^2\right] + \frac{\mu_2}{K_2 k_2}\left(u_2^2 + w_2^2\right) = 0 \tag{6}$$

where u_i and w_i are the primary and secondary velocity distributions corresponding to x and z directions, the coefficient of thermal expansion is β_i and T_i is the temperature. The no-slip condition is that the velocity must be vanishing at the wall. The corresponding boundary and interface conditions on primary and secondary velocity distributions are:

$$u_1(h_1)=0,\ w_1(h_1)=0;\ u_1(0)=u_2(0),\ \ w_1(0)=w_2(0);\ u_2(-h_2)=0,\ w_2(-h_2)=0 \tag{7}$$

$$\mu_1\frac{du_1}{dy}=\mu_2\frac{du_2}{dy} \text{ and } \mu_1\frac{dw_1}{dy}=\mu_2\frac{dw_2}{dy} \text{ at y=0.} \tag{8}$$

As the walls are maintained at varying temperatures T_{w1} and T_{w2}, the boundary conditions on T_1 and T_2 are:

$$T_1(0)=T_2(0), T_1(h_1)=T_{w1},\ T_2(-h_2)=T_{w2},\ K_1\frac{dT_1}{dy}=K_2\frac{dT_2}{dy}\ \ at\ \ y=0. \tag{9}$$

In making these equations dimensionless, the following transformations are used

$$\frac{u_1}{u_1}=u_1^*,\ \frac{u_2}{u_1}=u_2^*,\ \frac{w_1}{u_1}=w_1^*,\ \frac{w_2}{u_1}=w_2^*,\ y_1^*=\frac{y_1}{h_1},\ \frac{y_2}{h_2}=y_2^*,\ \left[\frac{(T-T_{w2})}{(T_{w1}-T_{w2})}\right]=\theta,\ Gr=\frac{g\,\beta_1\,h_1^{\,3}(T_{w1}-T_{w2})}{\nu_1^{\,2}},\ \mathrm{Re}=\frac{\bar{u}_1\,h_1}{\nu_1},\ R^2=\frac{\Omega\,h_1^{\,2}}{\nu},$$

$$K=\frac{K_1}{K_2},\ h=\frac{h_2}{h_1},\ n=\frac{\rho_2}{\rho_1},\ b=\frac{\beta_2}{\beta_1},\ \mathrm{Pr}=\frac{\mu_1 C_p}{K_1},\ \lambda=\frac{h_1}{\sqrt{k_1}},\ P=\left(\frac{h_1^{\,2}}{\mu_1\bar{u}_1}\right)\left(\frac{\partial p}{\partial x}\right),\ Ec=\frac{\bar{u}_1^{\,2}}{C_p(T_{w1}-T_{w2})},\ m=\frac{\mu_1}{\mu_2},k=\frac{k_1}{k_2}$$

Here $\bar{u}_1$ is average velocity.

Using the above transformations, the Equation (1) to Equation (6) transform to:

Region-I

$$\frac{d^2u_1}{dy^2}+\frac{Gr}{Re}(Sin\phi)\theta_1-\lambda^2u_1=P+2R^2w_1 \tag{10}$$

$$\frac{d^2w_1}{dy^2}-\lambda^2w_1=-2R^2u_1 \tag{11}$$

$$\frac{d^2\theta_1}{dy^2}+PrEc\left[\left(\frac{du_1}{dy}\right)^2+\left(\frac{dw_1}{dy}\right)^2\right]+PrEc\lambda^2\left(u_1^{\,2}+w_1^{\,2}\right)\Big)=0 \tag{12}$$

Region-II

$$\frac{d^2u_2}{dy^2}+\frac{Gr}{\mathrm{Re}}\,bmnh^2(Sin\phi)\theta_2-\ \lambda^2h^2ku_2=mh^2P+2R^2w_2 \tag{13}$$

$$\frac{d^2w_2}{dy^2}-\lambda^2h^2kw_2=-2R^2u_2 \tag{14}$$

$$\frac{d^2\theta_2}{dy^2}+\mathrm{Pr}\,Ec\frac{K}{m}\left[\left(\frac{du_2}{dy}\right)^2+\left(\frac{dw_2}{dy}\right)^2\right]+\ \mathrm{Pr}\,Eckh^2\lambda^2\frac{K}{m}(u_2^{\,2}+w_2^{\,2})=0 \tag{15}$$

The dimensionless forms of the boundary and interface conditions (8) and (9) change to:

$$u_1(1)=0,\ w_1(1)=0,\ u_1(0)=u_2(0),\ w_1(0)=w_2(0),\ u_2(-1)=0,\ w_2(-1)=0, \tag{16}$$

$$\frac{du_1}{dy}=\frac{1}{mh}\frac{du_2}{dy} \text{ and } \frac{dw_1}{dy}=\frac{1}{mh}\frac{dw_2}{dy} \text{ at y=0,} \tag{17}$$

$$\theta_1(1)=1,\ \theta_1(0)=\theta_2(0),\ \theta_2(-1)=0,\ \frac{d\theta_1}{dy}=\frac{1}{K\,h}\frac{d\theta_2}{dy}\ \ at\ \ y=0. \tag{18}$$

Writing $q_1 = u_1 + iw_1$ and $q_2 = u_2 + iw_2$, Equation (10) and Equation (15) can be written in complex form as:

Region-I

$$\frac{d^2q_1}{dy^2}+\frac{Gr}{\mathrm{Re}}(\sin\varphi)\theta_1-\lambda^2q_1=P-2i\,R^2q_1 \tag{19}$$

$$\frac{d^2\theta_1}{dy^2}+\Pr Ec\left[\frac{dq_1}{dy}\frac{d\bar{q}_1}{dy}\right]+\Pr Ec\lambda^2(q_1\bar{q}_1)=0. \tag{20}$$

Region-II

$$\frac{d^2q_2}{dy^2}+\frac{Gr}{\mathrm{Re}}bmnh^2(\sin\varphi)\theta_2-\lambda^2h^2kq_2=mh^2P-2i\,R^2q_2, \tag{21}$$

$$\frac{d^2\theta_2}{dy^2}+\Pr Ec\frac{K}{m}\left[\frac{dq_2}{dy}\frac{d\bar{q}_2}{dy}\right]+\Pr Ec\frac{K}{m}h^2k\lambda^2(q_2\bar{q}_2)=0 \tag{22}$$

$\bar{q}_1$ and $\bar{q}_2$ are the complex conjugates of q_1 and q_2 respectively.

The respective boundary and interface conditions are:

$$q_1(1)=0, q_1(0)=q_2(0), q_2(-1)=0, \frac{dq_1}{dy}=\frac{1}{mh}\frac{dq_2}{dy}\qquad at\ \ y=0, \tag{23}$$

$$\theta_1(1)=1, \theta_1(0)=\theta_2(0), \theta_2(-1)=0, \frac{d\theta_1}{dy}=\frac{1}{Kh}\frac{d\theta_2}{dy}\qquad at\ \ y=0, \tag{24}$$

2.1 Solutions of the problem

The governing equations are coupled and non-linear. Here, we consider the Eckert number to be very small. Hence, Pr.Ec (=ε) is also small and is used in the Perturbation Method. The solutions are considered in the following form

$$(q_i,\theta_i)=(q_{i0},\theta_{i0})+\varepsilon(q_{i1},\theta_{i1})+..... \tag{25}$$

where q_{i0},θ_{i0} are solutions for the case when ε is equal to zero and q_{i1},θ_{i1} are perturbed quantities related to q_{i0},θ_{i0} respectively. Substituting the above solutions in equations (19) to (22) and equating the factors of identical existing powers of ε, we obtain equations of zeroth-order and first-order approximations for Region I and Region II as follows:

Region I

Equations of zeroth-order approximation

$$\frac{d^2q_{10}}{dy^2}+\frac{Gr}{Re}(Sin\phi)\theta_{10}-\lambda^2q_{10}=P-2iR^2q_{10} \tag{26}$$

$$\frac{d^2\theta_{10}}{dy^2}=0 \tag{27}$$

Equations of first-order approximation

$$\frac{d^2q_{11}}{dy^2}+\frac{Gr}{Re}(Sin\phi)\theta_{11}-\lambda^2q_{11}=-2iR^2q_{11} \tag{28}$$

$$\frac{d^2\theta_{11}}{dy^2}+\left[\left(\frac{dq_{10}}{dy}\right)\left(\frac{d\bar{q}_{10}}{dy}\right)\right]+\lambda^2q_{10}\bar{q}_{10}=0 \tag{29}$$

The conjugate of q_{10} is $\bar{q}_{10}$

Region-II

Equations of zero[th]-order approximation

$$\frac{d^2q_{20}}{dy^2}+\frac{Gr}{\mathrm{Re}}\,bmnh^2(Sin\phi)\theta_{20}-\lambda^2h^2kq_{20}=mh^2P-2iR^2q_{20} \tag{30}$$

$$\frac{d^2\theta_{20}}{dy^2}=0 \tag{31}$$

Equations of first-order approximation

$$\frac{d^2q_{21}}{dy^2}+\frac{Gr}{Re}bmnh^2(Sin\phi)\theta_{21}-\lambda^2h^2kq_{21}=-2iR^2q_{21} \tag{32}$$

$$\frac{d^2\theta_{21}}{dy^2}+\frac{K}{m}\left[\left(\frac{dq_{20}}{dy}\frac{d\bar{q}_{20}}{dy}\right)\right]+\frac{K}{m}h^2k\lambda^2\left(q_{20}\bar{q}_{20}\right)=0 \tag{33}$$

The respective boundary conditions given in Equation (23) and (24) will be changed to:

$$q_{10}(1)=0,q_{10}(0)=q_{20}(0),q_{20}(-1)=0,\frac{dq_{10}}{dy}=\frac{1}{mh}\frac{dq_{20}}{dy}\qquad when\ y=0, \tag{34}$$

$$\theta_{10}(1)=1,\theta_{10}(0)=\theta_{20}(0),\theta_{20}(-1)=0,\frac{d\theta_{10}}{dy}=\frac{1}{Kh}\frac{d\theta_{20}}{dy}\qquad when\ y=0, \tag{35}$$

$$q_{11}(1)=0,q_{11}(0)=q_{21}(0),q_{21}(-1)=0,\frac{dq_{11}}{dy}=\frac{1}{mh}\frac{dq_{21}}{dy}\qquad when\ y=0, \tag{36}$$

$$\theta_{11}(1)=0,\theta_{11}(0)=\theta_{21}(0),\theta_{21}(-1)=0,\frac{d\theta_{11}}{dy}=\frac{1}{Kh}\frac{d\theta_{21}}{dy}\qquad when\ y=0, \tag{37}$$

It is noted that

$$q_{10}=u_{10}+i\,w_{10},\ q_{20}=u_{20}+iw_{20},\ q_{11}=u_{11}+i\,w_{11}\ \text{and}\ q_{21}=u_{21}+iw_{21}. \tag{38}$$

Solutions of equations of zeroth-order approximation (26), (27) and (30), (31) applying boundary conditions (34) and (35) are:

$$\theta_{10}=\frac{y+Kh}{1+Kh} \tag{39}$$

$$\theta_{20}=\frac{(y+1)Kh}{1+Kh} \tag{40}$$

$$u_{10}=[(c_1e^{(E_1y)}+c_2e^{(-E_1y)})cos(E_2y)+A_8+A_9y] \tag{41}$$

$$w_{10}=-[(c_1e^{(E_1y)}-c_2e^{(-E_1y)})\sin(E_2y)-A_{10}-A_{11}y] \tag{42}$$

$$u_{20}=[(c_3e^{(E_3y)}+c_4e^{-E_3y})cos(E_4y)+A_{16}+A_{17}y] \tag{43}$$

$$w_{20} = -[(c_3 e^{(E_3 y)} - c_4 e^{-E_3 y}) \sin(E_4 y) - A_{18} - A_{19} y] \tag{44}$$

Solutions of equations of first-order approximation (28), (29) and (32), (33) using boundary conditions (36) and (37) are:

$$\begin{aligned}\theta_{11} = \{&c_5 y + c_6 + D_{54} e^{E_1 y} \sin(E_2 y) + D_{55} e^{-E_1 y} \sin(E_2 y) + D_{56} e^{-E_1 y} \cos(E_2 y) + D_{57} e^{E_1 y} \cos(E_2 y) \\ &+ D_{58} y e^{E_1 y} \sin(E_2 y) + D_{59} y e^{-E_1 y} \cos(E_2 y) + D_{60} y e^{E_1 y} \cos(E_2 y) + D_{61} y e^{(-E_1 y)} \sin(E_2 y) \\ &+ D_{70} e^{(2E_1 y)} + D_{71} e^{(-2E_1 y)} + D_{72} 2\cos(2E_2 y) + D_7 3y^3 + D_7 4y^4 + D_7 5y^2\} \\ &+ i\{D_{76} sin(2E_2 y) + D_{62} e^{(E_1 y)} sin(E_2 y) + D_{63} e^{(E_1 y)} cos(E_2 y) + D_{64} e^{(-E_1 y)} \sin(E_2 y)\} \\ &+ i\{D_{65} e^{(-E_1 y)} \cos(E_2 y) + D_{66} y e^{(E_1 y)} cos(E_2 y) + D_{67} y e^{(E_1 y)} sin(E_2 y)\} \\ &+ i\{D_{68} y e^{(-E_1 y)} \cos(E_2 y) + D_{69} y e^{(-E_1 y)} sin(E_2 y)\}\end{aligned} \tag{45}$$

$$\begin{aligned}\theta_{21} = \{&c_9 y + c_{10} + J_{54} e^{E_3 y} \sin(E_4 y) + J_{55} e^{-E_3 y} \sin(E_4 y) + J_{56} e^{-E_3 y} \cos(E_4 y) + J_{57} e^{E_3 y} \cos(E_4 y) \\ &+ J_{58} y e^{E_3 y} \sin(E_4 y) + J_{59} y e^{-E_3 y} \cos(E_4 y) + J_{60} y e^{E_3 y} \cos(E_4 y) + J_{61} y e^{-E_3 y} \sin(E_4 y) \\ &+ J_{70} e^{2E_3 y} + J_{71} e^{-2E_3 y} + J_{72} \cos(2E_4 y) + J_{73} y^3 + J_{74} y^4 + J_{75} y^2\} \\ &+ i\{J_{76} sin(2E_4 y) + J_{62} e^{(E_3 y)} sin(E_4 y) + J_{63} e^{(E_3 y)} cos(E_4 y) + J_{64} e^{(-E_3 y)} sin(E_4 y)\} \\ &+ i\{J_{65} e^{(-E_3 y)} cos(E_4 y) + J_{66} y e^{(E_3 y)} cos(E_4 y) + J_{67} y e^{(E_3 y)} sin(E_4 y)\} \\ &+ i\{J_{68} y e^{(-E_3 y)} cos(E_4 y) + J_{69} y e^{(-E_3 y)} sin(E_4 y)\}\end{aligned} \tag{46}$$

$$\begin{aligned}u_{11} = &\left(c_7 e^{E_1 y} + c_8 e^{-E_1 y}\right) \cos(E_2 y) - P_5 e^{2E_1 y} - P_7 e^{-2E_1 y} + P_{75} + P_{76} y + P_{77} y^2 + P_{13} y^3 \\ &+ P_{17} y^4 + P_{23} \cos(2E_2 y) - P_{50} \sin(2E_2 y) + P_{78} e^{E_1 y} \cos(E_2 y) + P_{79} e^{E_1 y} \sin(E_2 y) \\ &+ P_{80} e^{-E_1 y} \cos(E_2 y) + P_{81} e^{-E_1 y} \sin(E_2 y) + P_{41} e^{E_1 y} y \cos(E_2 y) \\ &- P_{32} e^{E_1 y} y \sin(E_2 y) + P_{82} e^{-E_1 y} y \cos(E_2 y) + P_{83} e^{-E_1 y} y \sin(E_2 y) \\ &+ P_{84} e^{-E_1 y} y^2 \cos(E_2 y) + P_{85} e^{-E_1 y} y^2 \sin(E_2 y)\end{aligned} \tag{47}$$

$$\begin{aligned}w_{11} = &\left(c_8 e^{-E_1 y} - c_7 e^{E_1 y}\right) \sin(E_2 y) + P_6 e^{2E_1 y} + P_8 e^{-2E_1 y} + P_{86} + P_{87} y + P_{88} y^2 + P_{14} y^3 + P_{18} y^4 \\ &+ P_{24} \cos(2E_2 y) + P_{49} \sin(2E_2 y) + P_{89} e^{E_1 y} \cos(E_2 y) + P_{90} e^{E_1 y} \sin(E_2 y) \\ &+ P_{91} e^{-E_1 y} \cos(E_2 y) + P_{92} e^{-E_1 y} \sin(E_2 y) + P_{61} e^{E_1 y} y \cos(E_2 y) \\ &- P_{58} e^{E_1 y} y \sin(E_2 y) + P_{93} e^{-E_1 y} y \cos(E_2 y) + P_{94} e^{-E_1 y} y \sin(E_2 y) \\ &+ P_{95} e^{-E_1 y} y^2 \cos(E_2 y) + P_{96} e^{-E_1 y} y^2 \sin(E_2 y)\end{aligned} \tag{48}$$

$$\begin{aligned}u_{21} = &\left(c_{11} e^{E_3 y} + c_{12} e^{-E_3 y}\right) \cos(E_4 y) - F_5 e^{2E_3 y} - F_7 e^{-2E_3 y} + F_{75} + F_{76} y + F_{77} y^2 + F_{13} y^3 + F_{17} y^4 \\ &+ F_{23} \cos(2E_4 y) - F_{50} \sin(2E_4 y) + F_{78} e^{E_3 y} \cos(E_4 y) + F_{79} e^{E_3 y} \sin(E_4 y) \\ &+ F_{80} e^{-E_3 y} \cos(E_4 y) + F_{81} e^{-E_3 y} \sin(E_4 y) + F_{41} e^{E_3 y} y \cos(E_4 y) \\ &- F_{32} e^{E_3 y} y \sin(E_4 y) + F_{82} e^{-E_3 y} y \cos(E_4 y) + F_{83} e^{-E_3 y} y \sin(E_4 y) \\ &+ F_{84} e^{-E_3 y} y^2 \cos(E_4 y) + F_{85} e^{-E_3 y} y^2 \sin(E_4 y)\end{aligned} \tag{49}$$

$$\begin{aligned}w_{21} = &\left(c_{12} e^{-E_3 y} - c_{11} e^{E_3 y}\right) \sin(E_4 y) + F_6 e^{2E_3 y} + F_8 e^{-2E_3 y} + F_{86} + F_{87} y + F_{88} y^2 + F_{14} y^3 + F_{18} y^4 \\ &+ F_{24} \cos(2E_4 y) + F_{49} \sin(2E_4 y) + F_{89} e^{E_3 y} \cos(E_4 y) + F_{90} e^{E_3 y} \sin(E_4 y) \\ &+ F_{91} e^{-E_3 y} \cos(E_4 y) + F_{92} e^{-E_3 y} \sin(E_4 y) + F_{61} \cos(E_4 y) e^{E_3 y} y \\ &- F_{58} e^{E_3 y} y \sin(E_4 y) + F_{93} \cos(E_4 y) e^{-E_3 y} y + F_{94} e^{-E_3 y} y \sin(E_4 y) \\ &+ F_{95} e^{-E_3 y} y^2 \cos(E_4 y) + F_{96} e^{-E_3 y} y^2 \sin(E_4 y)\end{aligned} \tag{50}$$

For the sake of briefness, the constants involved in Equations (41) - (50) are not given. Solutions for the equations of zeroth-order and first-order approximations from Equations (26) - (33) are solved numerically by fixing the parameters n=1.5, Re=5, b=1 and P = -5. As the solutions for the equations of zeroth-order approximation are linear, the graphs for temperature distribution are drawn only for first-order approximations. This shows that the temperature distribution up to zeroth-order approximation is due to the conduction only. In the Figures 1-10, excluding the varying one, all other parameters are taken from the set (ϕ, h, Gr, R, m, k, K, λ) = (30°, 1, 5, 1, 0.5, 0.5, 1, 2).

3. Results and Discussion

By solving the differential equations analytically, approximate solutions for primary as well as secondary velocity and temperature distribution are acquired. Numerical values of these solutions are computed for various sets of parameters and the results are depicted graphically. Here we note that when the rotation R=0, these results are in agreement with that of Malashetty, Umavathi, and Kumar (2001).

Primary velocity distribution 'u' and secondary velocity distribution 'w' for different values of the rotation parameter R are shown in Figures 2(a) and 2(b) respectively.

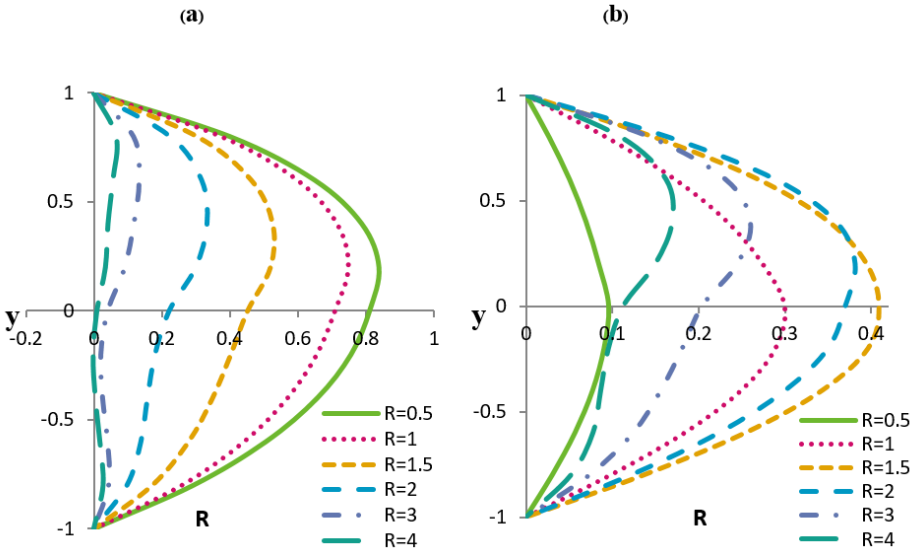

Figure 2. Velocity distribution of R (a) Primary (b) Secondary

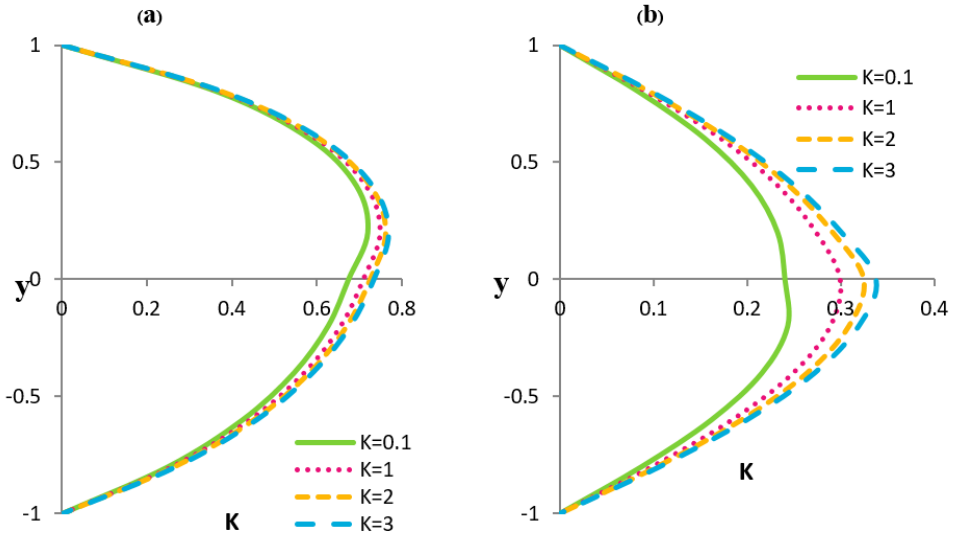

Figure 3. Velocity distribution of K (a) Primary (b) Secondary

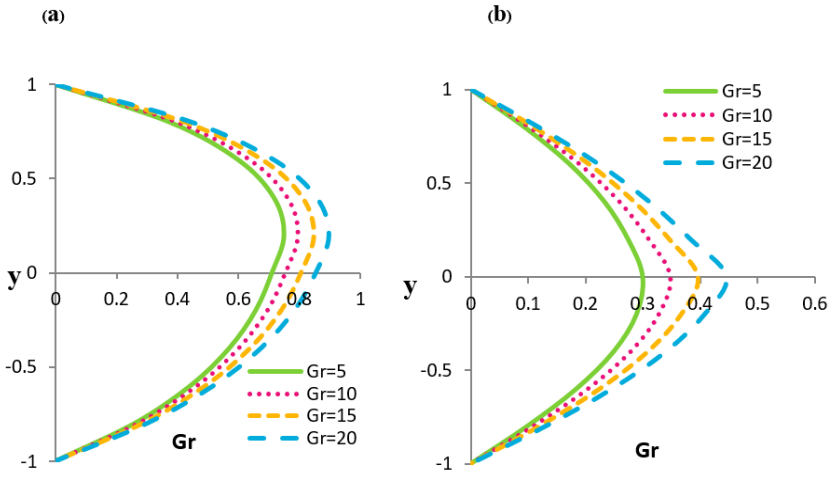

Figure 4. Velocity distribution of Gr (a) Primary (b) Secondary

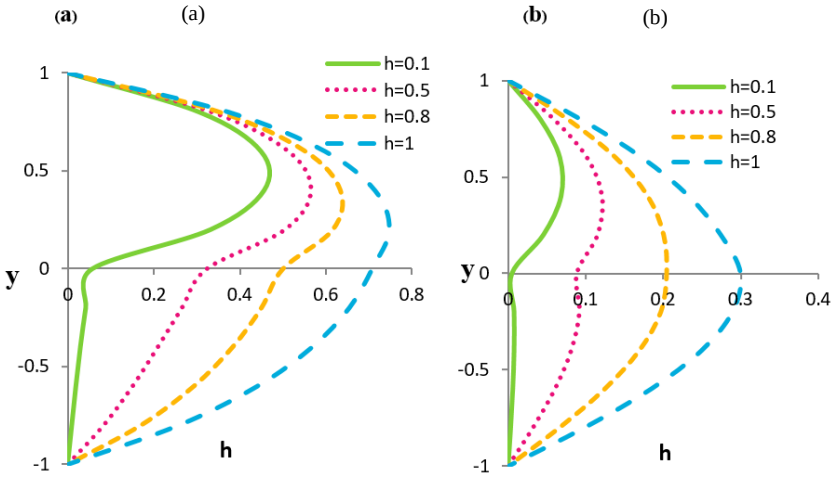

Figure 5. Velocity distribution of h (a) Primary (b) Secondary

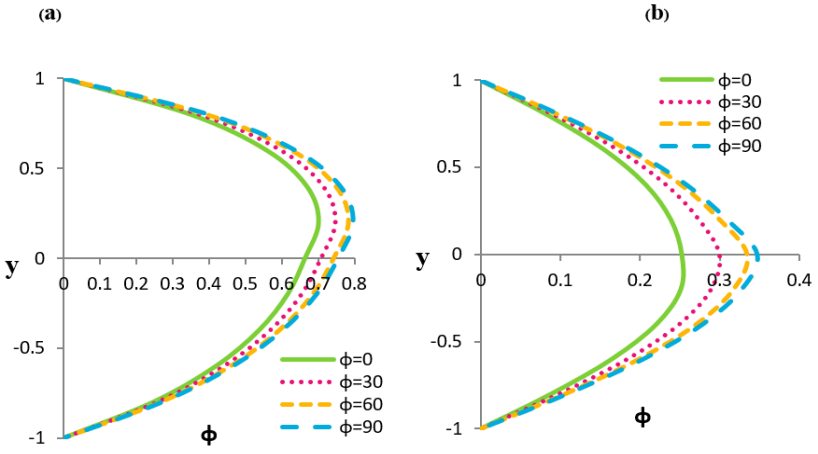

Figure 6. Velocity distribution of Ø (a) Primary (b) Secondary

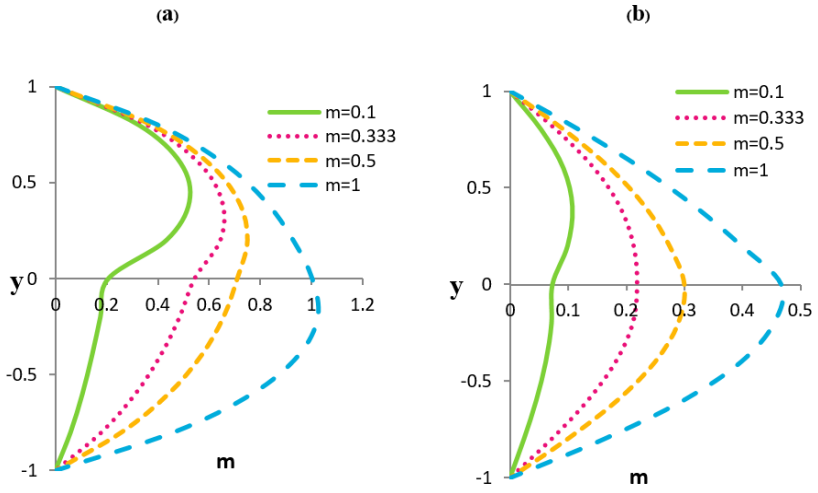

Figure 7. Velocity distribution of m (a) Primary (b) Secondary

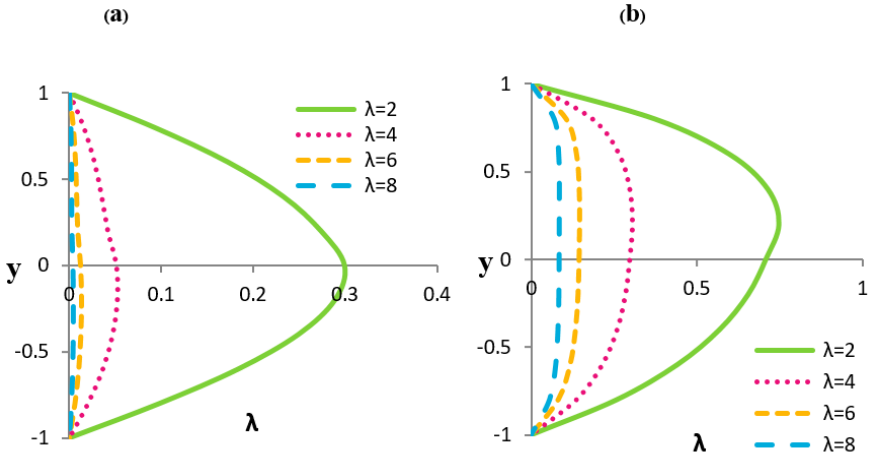

Figure 8. Velocity distribution of λ (a) Primary (b) Secondary

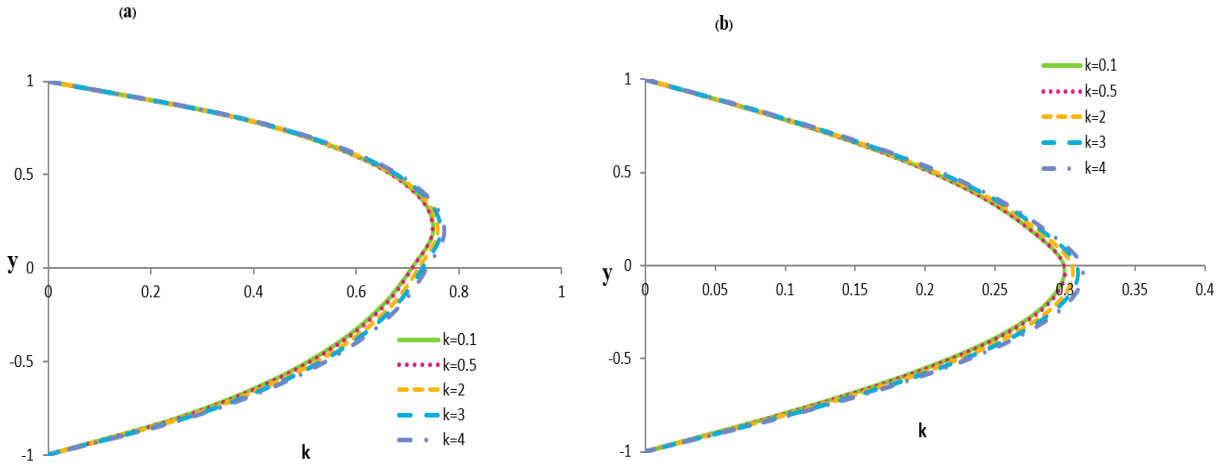

Figure 9. Velocity distribution of k (a) Primary (b) Secondary

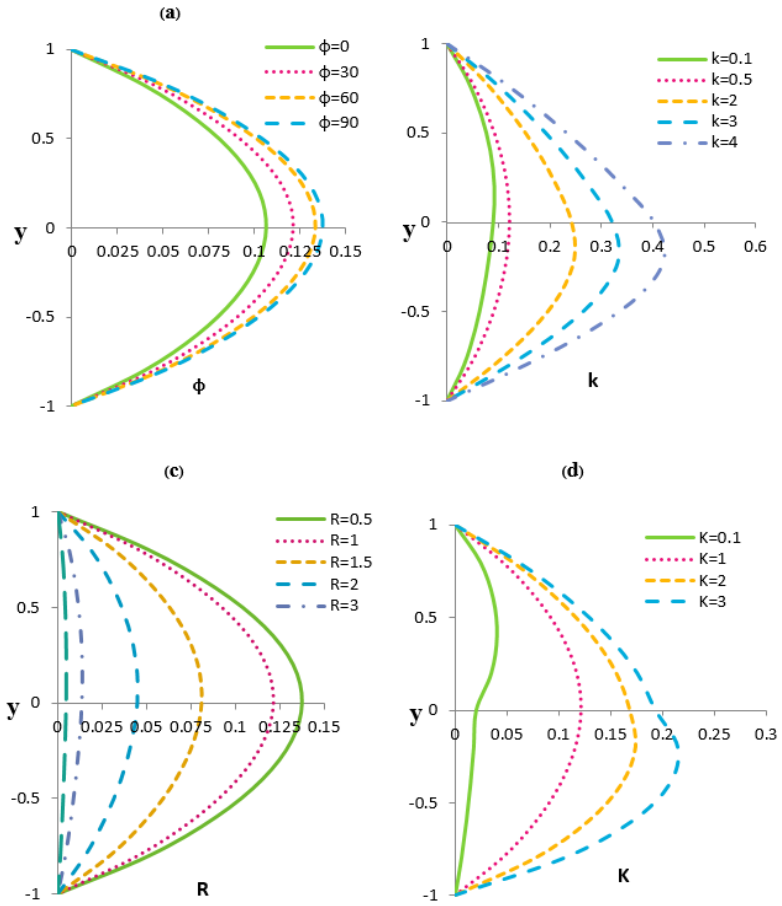

Figure 10(i). Temperature distribution of (a) Ø, (b) k, (c) R, (d) K

It is concluded that ‘u’ reduces with increasing rotation. Since R is the ratio of the Coriolis force and the viscous force, as R increases the Coriolis force also increases. The increasing Coriolis forces oppose the buoyancy force. Hence the velocity will be decreased. It is also concluded that as the rotation parameter R increases in (0, 1.6), the secondary velocity ‘w’ also increases, but outside the range as R increases, it decreases. The impact of the ratio on thermal conductivities K is shown in Figures 3(a) and 3(b). It is noticed that by increasing K there is a rise in the primary and secondary velocities. Figures 4(a) and 4(b) represent ‘u’ and ‘w’ for varied values of the Grashof number Gr. As Gr increases, both the velocities also increase with the rise in the value of Gr. The impact of the ratio of heights ‘h’ on ‘u’ and ‘w’ is depicted in Figures 5(a) and 5(b) respectively. The impact of increasing ‘h’ is to enhance both the velocities. The impact of the inclination angle ϕ on ‘u’ and ‘w’ is depicted in Figures 6(a) and 6(b) respectively. As the buoyancy force enhances with an increase in the inclination angle, both the primary as well as secondary velocities increase with the increasing values of ϕ. Figures 7(a) and 7(b) show the impact of the ratio of viscosities, ‘m’ on primary as well as secondary velocities, respectively. It is observed that by increasing ‘m’ there is an increase both in the primary and secondary velocities. Figures 8(a) and 8(b) represent the impact of porous parameter λ on primary as well as secondary velocities. It is observed that as the value of λ increases there is a decrease in both the velocities in two regions because of the drag caused by the porous matrix on the flow of the first region, which also affects the flow of the free viscous fluid phase. Also, it is noticed that the effect of greater λ on the velocity is more pronounced when compared to smaller λ. Figures 9(a) and 9(b) indicate the impact of permeability of porous medium k, showing that increased k increases both the primary and secondary velocities.

The impact of the angle of inclination ϕ on temperature θ is represented in Figure 10(a). The increased values of ϕ enhance the temperature because as ϕ increases the buoyancy force also increases. Figure 10(b) indicates the effect of permeability of the porous medium k on temperature θ, indicating a proportionate increase in heat transfer. Figure 10(c) represents the impact of R on θ, the temperature distribution. It is observed that the temperature reduces with an increase in rotation. As the rotation parameter R increases, the temperature decreases because increasing rotation increases the Coriolis force, which in turn opposes the buoyancy force. Thus, the velocity will be decreased, leading to a reduction in the temperature. Figure 10(d) indicates the effect of the ratio of thermal conductivities K on temperature θ; the larger the ratio of thermal conductivities, the greater the amounts of heat transfer. Figure 10(e) shows the impact of Gr on temperature

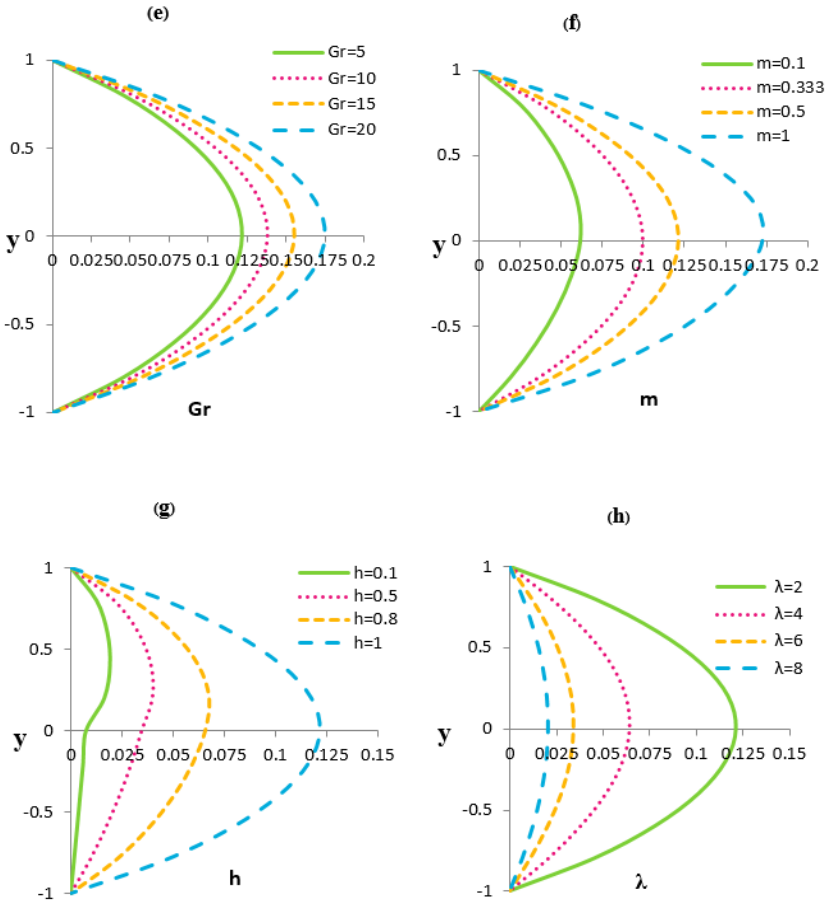

Figure 10(ii). Temperature distribution of (e) Gr, (f) m, (g) h, (h) λ

θ. It is noticed that with an increase in Gr there is also an increase in the temperature distribution. Figure 10(f) depicts the impact of the ratio of viscosities m on the temperature distribution. Increase in ratio of viscosities enhances the temperature of the flow. Figure 10(g) exhibits the effect of the ratio of heights h on the temperature θ; increasing the value of h increases the temperature. The effect of porous parameter λ on temperature distribution θ is shown in Figure 10(h). It is observed that similar to its effect on the fluid flow, an increasing value of λ decreases the temperature field.

4. Conclusions

It is noticed that the impact of the porous parameter is to retard the temperature, primary velocity and secondary velocity in both phases. The increase in buoyancy force incorporated through Grashof number and the angle of inclination enhances the temperature, primary velocity and secondary velocity for both the layers. The increase in Coriolis force incorporated through the rotation parameter reduces the temperature and primary velocity of the flow in both phases. The flow and thermal aspects of the fluids in the channel are enhanced by an increase in the ratio of viscosities of the fluids and the ratio of heights of the two phases. The results of the two-layered flow and temperature distribution through an inclined porous medium could be useful in recharge/discharge problems like the flow of geophysical fluids, packed-bed energy storage, etc.

References

Beckermann, C., Viskanta, R., & Ramadhyani, S. (1988). Natural convection in vertical enclosures containing simultaneously fluid and porous layers. *Journal of Fluid Mechanics*, *186*, 257-284.

Bian, W., Vasseur, P., Bilgen, E., & Meng, F. (1996). Effect of an electromagnetic field on natural convection in an inclined porous layer. *International Journal of Heat and Fluid Flow*, *17*(1), 36-44.

Chauhan, D. S., & Rashmi, A. (2010). Effect of Hall current on MHD flow in a rotating channel partially filled with a porous medium. *Chemical Engineering Communications*, *197*(6), 830-845.

Chauhan, D. S., & Rashmi, A. (2012a). Magnetohydrodynamic convection effects with viscous and Ohmic dissipation in a vertical channel partially filled by a porous medium. *Journal of Applied Science and Engineering*, *15*(1), 1-10.

Chauhan, D. S., & Rastogi, P. (2009). Hall current and heat transfer effects on MHD flow in a channel partially filled with a porous medium in a rotating system. *Turkish Journal of Engineering and Environmental Sciences, 33*(3), 167-184. doi:10.3906/muh-0905-6

Chauhan, D. S., & Rastogi, P. (2012). Heat transfer effects on rotating MHD Couette flow in a channel partially filled by a porous medium with Hall current. *Journal of Applied Science and Engineering, 15*(3), 281-290.

Chauhan, D. S., & Rema, J. (2005). Three-dimensional MHD steady flow of a viscous incompressible fluid over a highly porous layer. *Modelling, Measurement and Control B, 74*, 19-34.

Guven, K., Aytac, A., Ebru, T., & Ibrahim, O. (2010). Second-law analysis for an inclined channel containing porous-clear fluid layers by using the differential transform method. *An International Journal of Computation and Methodology, Numerical Heat Transfer, Part A: Applications, 57*, 603-623.

Guven, K., Aytac, A., & Ibrahim, O. (2012). Analysis of the magnetic effect on entropy generation in an inclined channel partiallyfilled with a porous medium. *An International Journal of Computation and Methodology, Numerical Heat Transfer, Part A: Applications, 61*, 786–799.

Hayat, T., Husain, M., & Khan, M. (2007). Effects of Hall current on flows of a Burger's fluid through a porous medium. *Transport Porous Media, 68*(2), 249-263.

Hayat, T., Maryiam, J., & Ali, N. (2008). MHD peristaltic transport of a Jeffery fluid in a channel with compliant walls and porous space. *Transport in Porous Media, 74*(3), 259-274.

Krishna, D. V., Prasad Rao, D. R. V., & Ramachandra Murthy, A. S. (2002). Hydromagnetic convection flow through a porous medium in a rotating channel. *Journal of Engineering Physics and Thermophysics, 75*(2), 281-291.

Kuznetsov, A. V. (1998). Analytical investigation of Couette flow in a composite channel partially filled with a porous medium and partially with a clear fluid. *International Journal of Heat and Mass Transfer, 41*(16), 2556-2560.

Lima, J. A., Assad, G. E., & Paiva, H. S. (2016). A simple approach to analyze the fully developed two-phase magnetoconvection type flows in inclined parallel-plate channels. *Latin American Applied Research, 46*, 93-98.

Malashetty, M. S., Umavathi, J. C., & Kumar, J. P. (2001). Convective flow and heat transfer in an inclined composite porous medium. *Journal of Porous Medium, 4*, 15-22.

Prasad, V. (1991). Convective flow interaction and heat transfer between fluid and porous layers. In S. Kakac¸, B. Kilkis, F. A. Kulacki, & F. Arinc (Eds.), *Convective Heat and Mass Transfer in Porous Media* (pp. 563–615). Dordrecht, The Netherlands: Kluwer Academic.

Rudraiah, N. (1984). Non-linear convection in a porous medium with convective acceleration and viscous force. *Arabian Journal for Science and Engineering, 9*(2), 153-167.

Rudraiah, N. (1988). Heat and mass transfer in composite materials, Presidential address, Section of Mathematics, Indian Science Congress, India.

Seddeek, M. A. (2002). Effects of magnetic field and variable viscosity on forced non-darcy flow about a flat plate with variable wall temperature in porous media in the presence of suction and blowing. *Journal of Applied Mechanics and Technical Physics, 43*(1), 13-17.

Simon, D., & Shagaiya, Y. D. (2013). Convective flow of two immiscible fluids and heat transfer with porous along an inclined channel with pressure gradient. *Research Inventy: International Journal of Engineering and Science, 2*(4), 12-18.

Siva Reddy, S., Chamkha Ali, J., & Anjan Kumar, S. (2017). Thermal-diffusion and diffusion-thermo effects on MHD natural convective flow through a porous medium in a rotating system with ramped temperature. *International Journal of Numerical Methods for Heat and Fluid Flow, 27*(11), 2451-2480.

Sri Ramachandra Murty, P., & Balaji Prakash, G. (2016). Magnetohydrodynamic two-fluid flow and heat transfer in an inclined channel containing porous and fluid layers in a rotating system. *Maejo International Journalof Science and Technology, 10*(1), 25-40.

Sri Ramachandra Murty, P., Balaji Prakash, G., & Karuna Sree, C. (2018). Rotating Hydromagnetic Two-Fluid Convective Flow and Temperature Distribution in an Inclined Channel. *International Journal of Engineering and Technology, 7*(4.10), *629-635*.

Sunil., & Mahajan, A. (2009). A nonlinear stability analysis for rotating magnetized ferrofluid heated from below saturating a porous medium. *The Journal of Applied Mathematics and Physics, 60*(2), 344-362.